Relationship between vertical shear rate and kinetic energy dissipation rate in stably stratified flows

David A. Hebert[1] and Stephen M. de Bruyn Kops[1]

Received 27 October 2005; revised 30 January 2006; accepted 2 February 2006; published 16 March 2006.

[1] High resolution direct numerical simulations of strongly stratified turbulence are analyzed in order to investigate the relationship between vertical shearing of horizontal motions and the dissipation rate of kinetic energy. The relative magnitude of each component of the dissipation rate is examined as a function of the Reynolds number and of the buoyancy Reynolds number. From the simulation results, in conjunction with published laboratory results, it is concluded that (1) the simulation results are consistent with the laboratory data but span a much larger range of buoyancy Reynolds number, (2) the ratio of the square of the vertical shear rate to the dissipation rate is a strong function of buoyancy Reynolds number, and (3) the approximation that vertical shear rate is the dominant cause of energy dissipation rate is only good when the buoyancy Reynolds number is less than order one. **Citation:** Hebert, D. A., and S. M. de Bruyn Kops (2006), Relationship between vertical shear rate and kinetic energy dissipation rate in stably stratified flows, *Geophys. Res. Lett.*, *33*, L06602, doi:10.1029/2005GL025071.

1. Introduction

[2] The dissipation rate of turbulent kinetic energy in the ocean is usually inferred from one or two components of the strain rate tensor. In the mixed region, isotropy is commonly assumed, [e.g., *Levine and Lueck*, 1999], but *Itsweire et al.* [1993] conclude that this approximation could lead to significantly underestimating the dissipation rate in strongly stratified flows. Another approximation that has been considered in the literature is that, in turbulence subject to strong stable stratification, the vertical shear of the horizontal motions causes most of the dissipation rate of kinetic energy, i.e.,

$$\nu S^2 \approx \varepsilon. \tag{1}$$

Here $\varepsilon = 2\nu e_{ij} e_{ij}$ is the kinetic energy dissipation rate, e_{ij} is the symmetric part of the viscous stress tensor, ν is the kinematic viscosity, and $S^2 = (\partial u/\partial z)^2 + (\partial v/\partial z)^2$, with u and v the horizontal components of velocity and z the vertical coordinate. *Riley and de Bruyn Kops* [2003] make approximation (1) in order to estimate a vertical length scale and *Billant and Chomaz* [2001] show that this approximation is consistent with their self-similarity analysis.

[3] Support for (1) comes from numerical simulations [e.g., *Herring and Métais*, 1989], and laboratory experiments that span a wide range of Reynolds numbers. In particular, the experiments of *Fincham et al.* [1996] show that $\nu S^2/\varepsilon \approx 0.9$, a result that is verified experimentally by *Praud et al.* [2005]. However, in terms of the buoyancy Reynolds number $\mathrm{Re}_b = \varepsilon/\nu N^2$ (where $N = \sqrt{-(g/\rho_0)(d\rho/dz)}$ is the buoyncy frequency), the data presented in both sets of experiments are with $\mathrm{Re}_b < 1$. In this paper, we consider a set of direct numerical simulations of strongly stratified turbulence that span more than two orders of magnitude in Reynolds number but also have buoyancy Reynolds numbers between about 0.1 and 15. In these simulations, (1) holds when $\mathrm{Re}_b \leq \mathcal{O}(1)$. For $\mathrm{Re}_b > 1$, the approximation deteriorates quickly with increasing Re_b so that when $\mathrm{Re}_b = 10$, $\nu S^2/\varepsilon \approx 0.4$.

[4] In order to understand when it is appropriate to make approximation (1), the results of the direct numerical simulations are presented with analysis of how the components of ε behave as functions of both the nominal and buoyancy Reynolds numbers. The simulation results are then shown to be consistent with and extend those obtained from the laboratory experiments cited above as well as those from other studies using direct numerical simulations. Before beginning the analysis, a brief description of the simulations is given in the next section.

2. Simulations

[5] The flows analyzed in this study are listed in Table 1, and are a superset of those reported by *Riley and de Bruyn Kops* [2003]. All flows have no mean shear and the linear background density gradient is constant in time and of sufficient magnitude to produce strong stable stratification. The initial condition for the simulations consisted of Taylor-Green vortices plus broad-banded noise with a level approximately 10% of the Taylor-Green vortex energy. The Froude number and Reynolds number characterizing the simulations are defined respectively as

$$\mathrm{F}_L = \frac{2\pi\mathcal{U}}{NL}, \quad \mathrm{Re}_L = \frac{\mathcal{U}L}{\nu}, \tag{2}$$

where $\mathcal{U}$ and L are initial velocity and length scales. Note that both the Froude and Reynolds numbers are defined in terms of the initial conditions, and so are merely nominal values used to identify the simulations.

[6] The flow fields are assumed to satisfy the incompressible continuity and Navier-Stokes equations subject to the Boussinesq approximation. A detailed description of the equations of motion, initial conditions, and numerical method are given by *Riley and de Bruyn Kops* [2003]. Also discussed in that paper is the fact that the simulated flows exhibit many characteristics of stratified

[1]Department of Mechanical and Industrial Engineering, University of Massachusetts Amherst, Amherst, Massachusetts, USA.

0094-8276/06/2005GL025071$05.00

Table 1. Conditions for Simulations of Quasi-Horizontal Vortices[a]

Notation	F_L	Re_L	$N_x = N_y$	N_z	Lx = Ly	Lz
F2R2	2	200	256	128	$4\pi\ L$	$2\pi\ L$
F2R4	2	400	256	128	$4\pi\ L$	$2\pi\ L$
F2R8	2	800	256	128	$4\pi\ L$	$2\pi\ L$
F2R16	2	1600	256	256	$4\pi\ L$	$4\pi\ L$
F2R32	2	3200	512	256	$4\pi\ L$	$2\pi\ L$
F2R64	2	6400	768	384	$4\pi\ L$	$2\pi\ L$
F2R96	2	9600	1024	512	$4\pi\ L$	$2\pi\ L$
F4R2	4	200	256	128	$4\pi\ L$	$2\pi\ L$
F4R4	4	400	256	128	$4\pi\ L$	$2\pi\ L$
F4R8	4	800	256	256	$4\pi\ L$	$4\pi\ L$
F4R16	4	1600	256	256	$4\pi\ L$	$4\pi\ L$
F4R32	4	3200	512	256	$4\pi\ L$	$2\pi\ L$
F4R64	4	6400	768	384	$4\pi\ L$	$2\pi\ L$
F4R96	4	9600	1024	512	$4\pi\ L$	$2\pi\ L$

[a] N_x, N_y, N_z are the number of grid points and L_x, L_y, L_z are domain size for each direction.

turbulence, for example, the horizontal length scales grow while the vertical length scales decrease in time. This, combined with decoupling of the horizontal motions in the vertical direction, leads to the formation of horizontal "pancake" vortices. This behavior is evident after a dimensionless time t of about 15. After about $t = 30$ the horizontal length scales in the flow are approaching the limit imposed by the size of the computational domain and so the simulations are stopped.

3. Results and Discussion

[7] We begin our analysis by considering the ratio $\nu\langle S^2\rangle/\langle\varepsilon\rangle$ for each of the cases in Table 1, shown in Figure 1, and each component $\langle\varepsilon_{ij}\rangle$ as a fraction of $\langle\varepsilon\rangle$, shown in Figure 2. Here $\langle\cdot\rangle$ denotes a volume averaged quantity. We consider first a snapshot in time at $t = 20$ since this is near the time when the turbulence kinetic energy peaks [*Riley and de Bruyn Kops*, 2003]. For $Re_L = 800$ at both $F_L = 2$ and 4, the results are entirely consistent with the experimental results of *Fincham et al.* [1996] and *Praud et al.* [2005] in that vertical shear accounts for about 90% of the dissipation rate. The horizontal shear terms are very small, as are the contributions to ε of the normal strain rates. There is some dissipation due to vertical motion, particularly in the $F_L = 4$ case, but it is small.

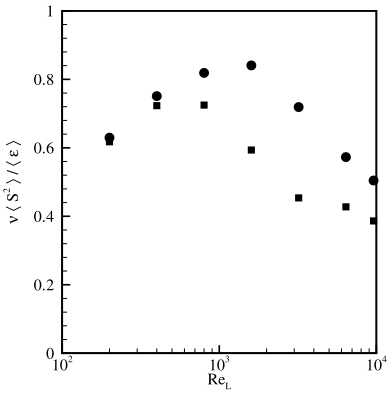

Figure 1. Ratio of $\nu\langle S^2\rangle/\langle\varepsilon\rangle$ vs. Re_L. $F_L = 2$ (solid circles): $F_L = 4$ (solid squares).

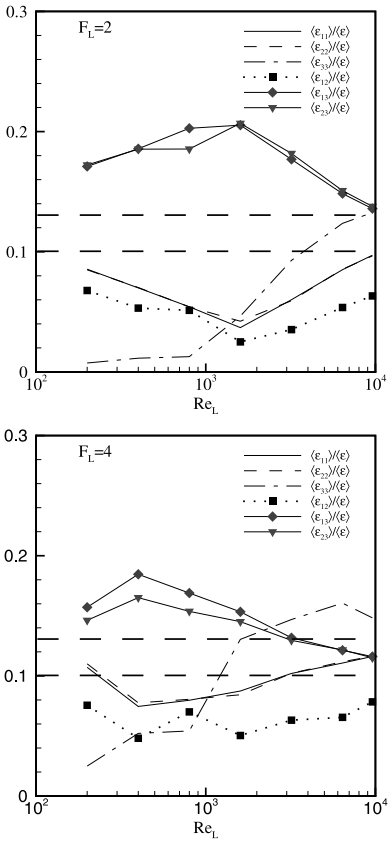

Figure 2. Contribution of the six independent terms of $\langle\varepsilon_{ij}\rangle$ normalized by $\langle\varepsilon\rangle$ vs. Re_L. (top) $F_L = 2$: (bottom) $F_L = 4$. The horizontal dashed lines mark the theoretical values for the normal and shear components in isotropic turbulence.

[8] For $Re_L = 200$, the flow conditions are markedly different with $\nu\langle S^2\rangle/\langle\varepsilon\rangle \approx 0.6$. The contributions of each component of $\langle\varepsilon\rangle$ are tending toward isotropy, except the vertical motions are suppressed by gravity. This can be seen by the increase in $\langle\varepsilon_{11}\rangle/\langle\varepsilon\rangle$ and $\langle\varepsilon_{22}\rangle/\langle\varepsilon\rangle$ compared to their values at $Re_L = 800$. Note that in fully isotropic turbulence, the contributions to $\langle\varepsilon\rangle$ of the diagonal terms in the strain rate tensor are 13.3%, while those of the off-diagonal terms are 10%.

[9] In the simulations with very low Reynolds number, the initial Taylor-Green condition remains almost undisturbed and the flow decays due to viscous effects, which suggests that the isotropic pressure force is strongly influencing the isotropic character of the flow. Note that these simulations do not represent that case when viscous effects become important after decay of a turbulent flow such as considered by *Fincham et al.* [1996] and *Praud et al.* [2005]. For the case of pancake vortices in strongly stratified viscous flows, *Godoy-Diana et al.* [2004] provide a detailed analysis.

[10] For Reynolds numbers above 800, the relative contributions of each component of $\langle\varepsilon\rangle$ change rapidly with increasing Re_L. Physical reasoning suggests that as the flow becomes more turbulent, the vertical velocity will increase as well as all components of $\langle\varepsilon\rangle$ that depend on vertical motions. Furthermore, such reasoning suggests that this

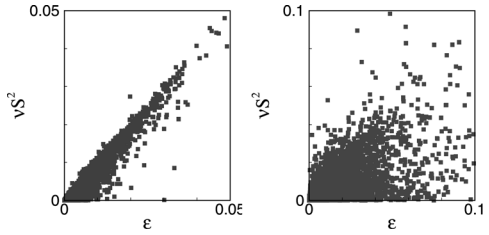

Figure 3. Scatterplot of νS^2 vs. ε for (left) F2R8 and (right) F2R64 at $t = 20$.

phenomenon will occur at lower Re_L for the $\mathrm{F}_L = 4$ cases than for the $\mathrm{F}_L = 2$ cases, since the vertical motions are more strongly suppressed by gravity at lower Froude numbers. The simulation data is consistent with this reasoning in that $\langle\varepsilon_{33}\rangle/\langle\varepsilon\rangle$ increases with Reynolds number for both $\mathrm{F}_L = 2$ and 4 and is higher for the $\mathrm{F}_L = 4$ cases except at the highest Reynolds numbers. Considering this result alone, we might conclude that the simulated flow is insufficiently stratified for (1) to hold for the higher Reynolds number cases. Note, however, the curves for $\langle\varepsilon_{11}\rangle$ and $\langle\varepsilon_{22}\rangle$ in Figure 2. The significant rise of these two contributions to $\langle\varepsilon\rangle$ shows that it is not just increasing vertical motion that causes $\nu\langle S^2\rangle/\langle\varepsilon\rangle$ to decrease to about 0.4 at $\mathrm{Re}_L = 9600$. Dissipation due to normal strains contributes significantly to the total dissipation rate at higher Reynolds numbers.

[11] Even though the ratio $\nu\langle S^2\rangle/\langle\varepsilon\rangle$ has been shown to decrease as Re_L increases, for most modeling and theoretical applications introduction of an order one constant would be acceptable provided that S^2 and ε were well correlated. This

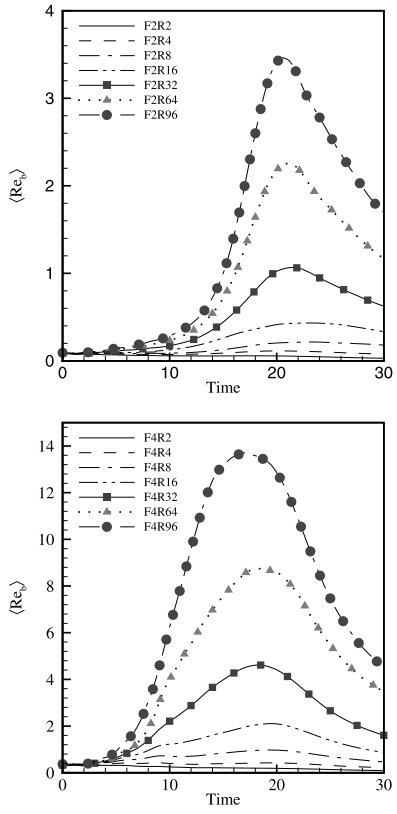

Figure 4. $\langle\mathrm{Re}_b\rangle$ vs. time for each simulation listed in Table 1.

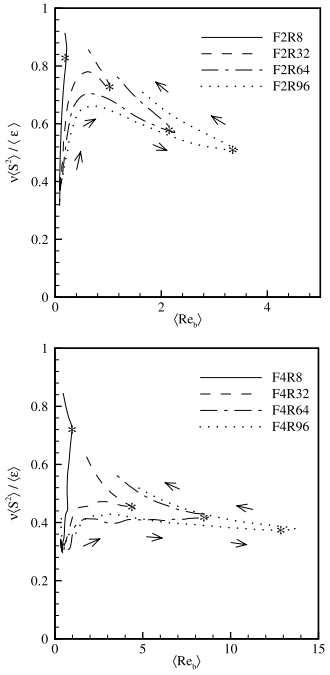

Figure 5. $\nu\langle S^2\rangle/\langle\varepsilon\rangle$ vs. $\langle\mathrm{Re}_b\rangle$ for several flow conditions for (top) $\mathrm{F}_L = 2$ and (bottom) $\mathrm{F}_L = 4$. The arrows indicate the direction of increasing time. Asterisks denote $t = 20$.

correlation is considered in Figure 3, in which local values of νS^2 are plotted versus ε for two different simulation cases at randomly selected points throughout the simulation domain. In Figure 3 (top), it is apparent that for $\mathrm{Re}_L = 800$ not only are the square of the shear and the dissipation rate well correlated, but there are very few points far from the diagonal. For this case, relation (1) is not only excellent on average, it is excellent locally in regions of high shear. In the bottom panel of the figure, the results for $\mathrm{Re}_L = 6400$ show that relation (1) is not very good even to within a multiplicative constant for this case.

[12] In order to understand why laboratory experiments conducted over a wide range of Reynolds numbers consistently show $\nu\langle S^2\rangle/\langle\varepsilon\rangle \approx 0.9$ while our simulations support this relationship only for a fairly narrow range of Reynolds numbers, we consider now both laboratory and simulation data in terms of the buoyancy Reynolds number. This quantity has been used extensively in the parameterization of stratified turbulence, [e.g., *Gibson*, 1980; *Gregg*, 1987; *Smyth and Moum*, 2000a; *Imberger and Boashash*, 1986] and can be derived from the ratio of the Ozmidov scale $L_\mathrm{O} = (\varepsilon/N^3)^{\frac{1}{2}}$ to the Kolmogorov scale $L_\mathrm{K} = (\nu^3/\varepsilon)^{\frac{1}{4}}$:

$$\mathrm{Re}_b = \left(\frac{L_\mathrm{O}}{L_\mathrm{K}}\right)^{\frac{4}{3}} = \frac{\varepsilon}{\nu N^2}. \tag{3}$$

The volume averaged buoyancy Reynolds number, $\langle\mathrm{Re}_b\rangle = \langle\varepsilon\rangle/\nu N^2$, for each simulation is plotted versus time in Figure 4, where $\langle\mathrm{Re}_b\rangle$ can be seen to increase up to about $t = 20$ and then to decrease. This is in agreement with the results of *Riley and de Bruyn Kops* [2003], in which shearing is shown to increase as the flow evolves, providing a source of energy to overcome the stratifica-

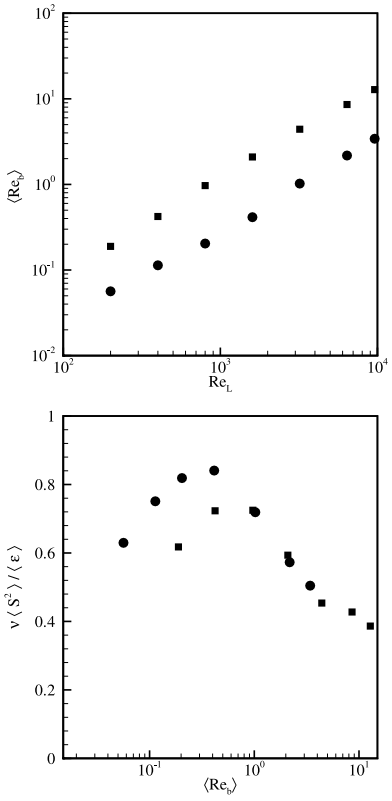

Figure 6. (top) $\langle \mathrm{Re}_b \rangle$ vs. Re_L and (bottom) $\nu\langle S^2 \rangle / \langle \varepsilon \rangle$ vs. $\langle \mathrm{Re}_b \rangle$ for $\mathrm{F}_L = 2$ (solid circles); $\mathrm{F}_L = 4$ (solid squares).

tion and promote the formation of turbulence, particularly at high Re_L. After $t = 20$, the turbulence (and hence $\langle \mathrm{Re}_b \rangle$) begin to decay.

[13] In Figure 5 is shown a plot of $\nu\langle S^2 \rangle / \langle \varepsilon \rangle$ versus $\langle \mathrm{Re}_b \rangle$ for some of the simulation cases over the entire simulation time. Recall that the simulations are initialized with the theoretical Taylor-Green configuration, and so no conclusions are drawn from the results at early times before the turbulence has developed, but they are provided for completeness. At time $t = 0$ the ratio of vertical shear to dissipation rate begins near 0.3 for all simulations. As the flow evolves, both $\nu\langle S^2 \rangle / \langle \varepsilon \rangle$ and Re_b increase until the point when Re_b approaches one. After this, $\nu\langle S^2 \rangle / \langle \varepsilon \rangle$ decreases with increasing Re_b, indicating the decreasing dominance of vertical shear in the dissipation rate, until Re_b reaches a maximum, corresponding to $t = 20$. At this point in the simulation, the turbulence begins to decay, Re_b decreases, and a corresponding increase $\nu\langle S^2 \rangle / \langle \varepsilon \rangle$ occurs. It is interesting that $\nu\langle S^2 \rangle / \langle \varepsilon \rangle$ is different during the portion of the simulations in which Re_b is increasing than during the portion in which it is decreasing. This indicates that not only is a measure of the instantaneous turbulence, such as Re_b, required to predict $\nu\langle S^2 \rangle / \langle \varepsilon \rangle$, but that the history of the flow is also important. In the context of the current paper, however, it is clear that Re_b has a strong effect on $\nu\langle S^2 \rangle / \langle \varepsilon \rangle$ and that (10 only holds for low values of Re_b.

[14] Figure 6 contains plots of Re_b vs. Re_L (upper plot) and $\nu\langle S^2 \rangle / \langle \varepsilon \rangle$ vs. Re_b (lower plot) at $t = 20$. When $\langle \mathrm{Re}_b \rangle > 1$, the data for both F_L cases collapse very well onto a common curve that decreases rapidly with increasing $\langle \mathrm{Re}_b \rangle$. In the range $0.1 < \langle \mathrm{Re}_b \rangle < 1$, there is more scatter in the data but high values of $\nu\langle S^2 \rangle / \langle \varepsilon \rangle$ are observed, consistent with results of other numerical simulations [e.g., *Smyth and Moum*, 2000b] as well as the laboratory results of *Fincham et al.* [1996] and *Praud et al.* [2005].

[15] For the case of *Fincham et al.* [1996] with $\mathrm{Re}_M = 6100$ and $N = 2.3$ rad s^{-1} used in their Figure 8 to show the contribution of vertical shear to dissipation rate, the buoyancy Reynolds number is estimated to be about 0.2 at early time. For the case of *Praud et al.* [2005] with $\mathrm{Re}_M = 9000$ and $\mathrm{Fr}_M = 0.09$ used in their Figure 25, the buoyancy Reynolds number is estimated to be about 0.1 at early time. These values of Re_b correspond roughly to where $\nu\langle S^2 \rangle / \langle \varepsilon \rangle$ is maximum in Figure 6.

[16] In both laboratory experiments, ε decreases by several orders of magnitude over the duration of the experiment with a corresponding decrease in buoyancy Reynolds number. Neither *Fincham et al.* [1996] nor *Praud et al.* [2005] report a decrease in $\nu S^2/\varepsilon$ as the experiments evolved, suggesting the data at low $\langle \mathrm{Re}_b \rangle$ in Figure 6 should be near 0.9 rather than the 0.6–0.8 reported here. These lower values are likely a result of these simulated flows being laminar, and thus never reaching a turbulent state. It is therefore likely, based on physical reasoning and the two sets of laboratory data, that vertical shear will account for 90% of the dissipation rate when $\langle \mathrm{Re}_b \rangle$ is order one or less provided that the flows are turbulent (of course, with $\langle \mathrm{Re}_b \rangle < 1$, turbulence is in the quasi-2d sense).

4. Conclusions

[17] Direct numerical simulations of strongly stratified flows are conducted for a range of Reynolds and Froude numbers and unity Schmidt number. The simulations span about two orders of magnitude in buoyancy Reynolds number. It is found that the contribution of vertical shear to the total dissipation rate of kinetic energy is a strong function $\langle \mathrm{Re}_b \rangle$. The simulation results, taken in conjunction with the laboratory experiments of *Fincham et al.* [1996] and *Praud et al.* [2005], indicate that the relation $\nu\langle S^2 \rangle / \langle \varepsilon \rangle \approx 0.9$ only applies when $\langle \mathrm{Re}_b \rangle$ is order one or less. For higher values of $\langle \mathrm{Re}_b \rangle$, normal strains make a significant contribution to $\langle \varepsilon \rangle$ and $\langle S^2 \rangle$ is not well correlated with $\langle \varepsilon \rangle$.

[18] A related question to that considered in this paper is, given measurements of one or two components of the strain rate in the ocean, how accurately can the kinetic energy dissipation rate be estimated? *Itsweire et al.* [1993] use DNS results to conclude that models used to predict ε based on streamwise velocity gradients will under-predict the true value by as much as a factor of 7. Figure 2, in which the streamwise components of the dissipation rate are shown to be lower than the isotropic value, supports this conclusion. *Smyth and Moum* [2000b], also using DNS results, conclude that the isotropic approximation is good provided that the buoyancy Reynolds number is high, a result that is consistent with the findings of *Gargett et al.* [1984] based on analysis of ocean data.

[19] **Acknowledgments.** This research is funded by the U.S. Office of Naval Research Grant N00014-04-1-0687. Grants of high performance computer time were provided by the Arctic Region Supercomputing Center and the U.S. Army Engineer Research and Development Center.

References

Billant, P., and J. M. Chomaz (2001), Self-similarity of strongly stratified inviscid flows, *Phys. Fluids*, *13*, 1645–1651.

Fincham, A. M., T. Maxworthy, and G. R. Spedding (1996), Energy dissipation and vortex structure in freely decaying, stratified grid turbulence, *Dyn. Atmos. Oceans*, *23*, 155–169.

Gargett, A., T. Osborn, and P. Nasmyth (1984), Local isotropy and the decay of turbulence in a stratified fluid, *J. Fluid Mech.*, *144*, 231–280.

Gibson, C. H. (1980), Fossil turbulence, salinity, and vorticity turbulence in the ocean, in *Marine Turbulence*, edited by J. C. Nihous, pp. 221–257, Elsevier, New York.

Godoy-Diana, R., J. M. Chomaz, and P. Billant (2004), Vertical length scale selection for pancake vorticies in strongly stratified viscous fluids, *J. Fluid Mech.*, *504*, 229–238.

Gregg, M. C. (1987), Diapycnal mixing in the thermocline—A review, *J. Geophys. Res.*, *92*, 5249–5286.

Herring, J. R., and O. Métais (1989), Numerical experiments in forced stably stratified turbulence, *J. Fluid Mech.*, *202*, 97–115.

Imberger, J., and B. Boashash (1986), Application of the winger-ville distribution to temperature gradient microstructure: A new technique to study small-scale variations, *J. Phys. Oceanogr.*, *16*, 1997–2012.

Itsweire, E. C., J. R. Koseff, D. A. Briggs, and J. H. Ferziger (1993), Turbulence in stratified shear flows: Implications for interpreting shear-induced mixing in the ocean, *J. Phys. Oceanogr.*, *23*, 1508–1522.

Levine, E. R., and R. G. Lueck (1999), Turbulence measurement from an autonomous underwater vehicle, *J. Atmos. Oceanic Technol.*, *16*, 1533–1544.

Praud, O., A. M. Fincham, and J. Sommeria (2005), Decaying grid turbulence in a strongly stratified fluid, *J. Fluid Mech.*, *522*, 1–33.

Riley, J. J., and S. M. de Bruyn Kops (2003), Dynamics of turbulence strongly influenced by buoyancy, *Phys. Fluids*, *15*, 2047–2059.

Smyth, W. D., and J. N. Moum (2000a), Length scales of turbulence in stably stratified mixing layers, *Phys. Fluids*, *12*, 1327–1342.

Smyth, W. D., and J. N. Moum (2000b), Anisotropy of turbulence in stably stratified mixing layers, *Phys. Fluids*, *12*, 1343–1362.

D. A. Hebert and S. M. de Bruyn Kops, Department of Mechanical and Industrial Engineering, University of Massachusetts Amherst, Amherst, MA 01003, USA. (dhebert@engin.umass.edu)